Energy straggling of ^{4}He ions below 2.0 MeV in Al, Ni, and Au†

J. M. Harris and M-A. Nicolet
California Institute of Technology, Pasadena, California 91125
(Received 15 July 1974; revised manuscript received 14 October 1974)

Energy straggling of ^{4}He ions has been measured in thin films of Ni, Al, and Au. The observed straggling is roughly proportional to the square root of thickness and appears to have a slight energy dependence for all these materials. The results are compared with predictions of the theories of Bohr, Lindhard and Scharff, and of Chu and Mayer. Both the Ni and Au results are below the predictions of Bohr and are above the predictions of Chu and Mayer, and of Lindhard and Scharff. The Al measurements are above predictions of all these theories.

INTRODUCTION

In recent years, backscattering spectrometry has been remarkably successful as a microanalytical tool for sensing mass, resolving depth, and perceiving monocrystalline structure in solids.[1] Energy straggling of the incident beam as it penetrates the target limits the ultimate ability to resolve depth. To estimate these limits, the magnitude of energy straggling must be known. Energy straggling depends on target material, beam energy, and incident particle. He and H are the most common projectiles used for backscattering analysis in the energy range of 1–2 MeV. Experimental straggling data in solids are available for H,[2] but those for He are much more scarce.[3–6] Pt is the only element for which He straggling measurements below 2.0 MeV in thin films exist.[6] Yet this is just the region where backscattering spectrometry is typically used. Measurements of ^{4}He$^+$ energy straggling below 2.0 MeV made in thin Al, Ni, and Au films are reported here. These materials were selected as representative of light, medium, and heavy elements.

ANALYTICAL METHOD

Energy straggling results from the statistical nature of the energy-loss processes a particle experiences as it penetrates matter. If $f(E)$ denotes the energy distribution function at some depth of an initially monoenergetic beam, then energy straggling Ω is defined as the standard deviation of $f(E)$ with respect to the average. This distribution function, in general, is rather complicated and nonsymmetrical with respect to the mean.[7] However, $f(E)$ has been measured for thin targets and in this case found to be approximately a Gaussian function of energy.[6] For analysis of the present data, $f(E)$ is thus assumed to be Gaussian. The standard deviation Ω of a Gaussian is related to the full width at half-maximum (FWHM). The FWHM of $f(E)$, ΔE, is given by

$$\Delta E = (8 \ln 2)^{1/2} \Omega = 2.355 \Omega. \quad (1)$$

In experimental work ΔE is the quantity usually determined, whereas theories normally predict values for Ω.

Traditionally, energy straggling was measured by transmission of a monoenergetic beam of particles through a self-supporting thin foil or gas cell. In this configuration $f(E)$ is measured from the energy spectrum of the transmitted beam and Ω determined directly. This method relies on thin highly uniform self-supported films which are difficult to produce and handle. These problems are circumvented by measuring in a backscattering configuration, because the film can be deposited on a rigid substrate. The experiments reported here were performed in this configuration.

Measurements made in backscattering, however, are more complicated to interpret for two reasons: (i) The beam traverses the target more than once, and (ii) the particle energy distribution function is modified by the backscattering collision. To interpret straggling measurements made by backscattering one should first consider the straggling of a beam traversing two layers in succession. The resulting straggling is $(\Omega_A^2 + \Omega_B^2)^{1/2}$, where Ω_A and Ω_B are the straggling measured at the appropriate energies for layers A and B individually, and where the distributions are assumed to be Gaussian. In the backscattering configuration, Ω_B simply corresponds to the straggling generated in the outgoing path, Ω_{out}. The straggling generated in the incoming path, Ω_{in}, must be modified, since this path terminates with an elastic collision. It can be shown that the standard deviation of any particle energy distribution function is multiplied by K after an elastic collision, where K is the elastic-scattering factor. The straggling in backscattering configuration Ω_b is thus given by

$$\Omega_b^2 = K^2 \Omega_{in}^2 + \Omega_{out}^2. \quad (2)$$

In practice, the incident beam is not monoenergetic but has an energy profile with standard deviation Ω_{beam}. Furthermore, the fluctuations in the detection system can be characterized by a standard

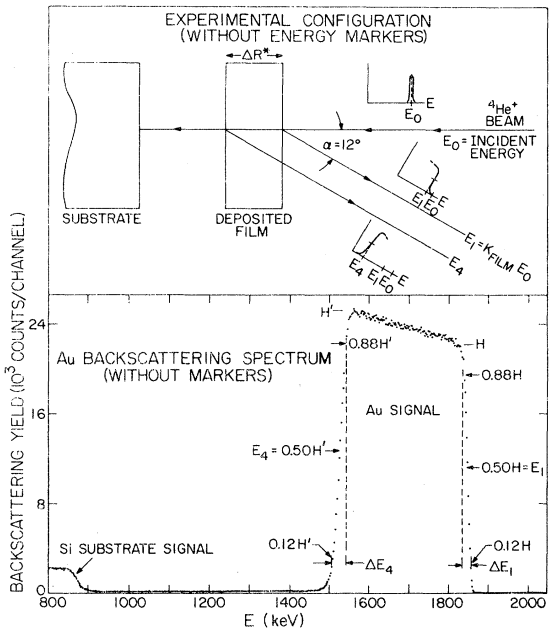

FIG. 1. Experimental configuration without energy markers and a typical backscattering spectrum of a Au target using $^4He^+$ ions and a solid-state detector.

deviation Ω_{det}. Both these standard deviations result from distributions which are closely Gaussian, so that the measured straggling value in backscattering configuration, Ω_4 is given by

$$\begin{aligned}\Omega_4^2 &= K^2(\Omega_{in}^2 + \Omega_{beam}^2) + \Omega_{out}^2 + \Omega_{det}^2 \\ &= K^2\Omega_{in}^2 + \Omega_{out}^2 + \Omega_1^2 \\ &= \Omega_b^2 + \Omega_1^2 \ , \end{aligned} \tag{3}$$

where Ω_1^2 is the system resolution, given by

$$\Omega_1^2 = K^2\Omega_{beam}^2 + \Omega_{det}^2 \ .$$

Equation (3) can be expressed equivalently as

$$\Omega_b = (1/2.355)(\Delta E_4^2 - \Delta E_1^2) \ , \tag{4}$$

where ΔE_4 and ΔE_1 are the FWHM associated with Ω_4 and Ω_1.

For films of heavy monoisotopic and inert elements such as Au, ΔE_1 and ΔE_4 can be obtained from the backscattering spectrum taken on a target consisting simply of the film and an appropriate substrate. ΔE_1 is obtained from the high-energy edge of the spectrum, since this signal originates from that fraction of the beam which scatters from the surface ($\Omega_{in} = 0 = \Omega_{out}$). Similarly, ΔE_4 can be obtained from the low-energy edge of the spectrum, since this signal is due to particles which traverse the film completely (see Fig. 1). These edges display the integrals of the energy distrubution functions associated with ΔE_1 and ΔE_4, respectively. Since these functions are assumed to be Gaussians, ΔE_1 and ΔE_4 are the energy differences between the 12 and 88% points of the front and rear edges. (See Fig. 1 and Ref. 6 for further details.)

In films of low atomic weight the backscattered particles lose a significant fraction of their energy in the elastic collision. The incoming and outgoing particles thus lie in separate energy ranges, which complicates the interpretation of the measurement. This difficulty can be removed by using targets with energy markers. These markers are very thin layers of heavy metal such as Pt or Au which are vacuum deposited on both sides of the film under investigation. To be usable as a marker, a layer of heavy element must be so thin that the energy loss of the beam traversing it is small compared to ΔE_1. When this is so, the system resolution function and the energy profile of the backscattered beam, as sampled by the heavy element, will be displayed by the backscattering signals of the top and bottom markers, respectively. ΔE_1 and ΔE_4 can then be measured from these marker signals directly (see Fig. 2). Whether a marker is thin enough can be easily tested. As discussed above, ΔE_1 can be obtained from the leading edge of a backscattering signal of a heavy element such as Au. Consequently, a marker is sufficiently thin if it indicates a system resolution Ω_1 (or ΔE_1) which is indistinguishable from that measured on the high-energy edge of a clean Au target. All our heavy markers meet this criterion and have typically an areal density of about 6 $\mu g/cm^2$.

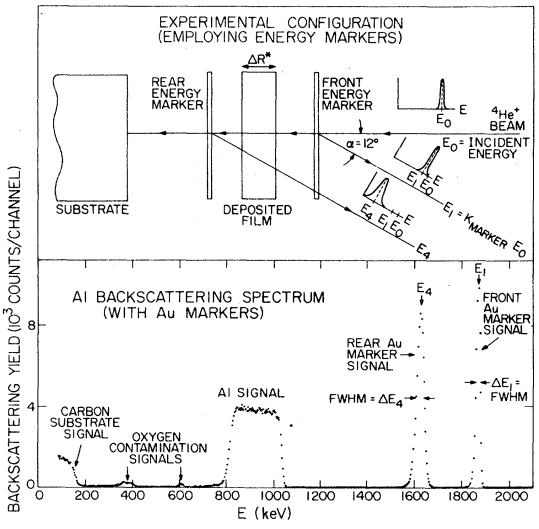

FIG. 2. Experimental configuration using energy markers and a typical backscattering spectrum of an Al dummy target using $^4He^+$ ions and a solid-state detector. Au energy markers and the target contamination level can be seen in the spectrum.

The beam loses energy both while traversing the film and during the backscattering collision. Therefore the straggling obtained is from a beam which has undergone energy loss. But since heavy markers were used for light elements, the incoming and outgoing particles lie in contiguous energy ranges and the measured straggling can be regarded as that observed for an average energy over the total path. The average energy chosen here, $\bar{E}$, is the same one used in calculating the stopping cross section $\epsilon_\alpha(\bar{E})$ from a backscattering spectrum and is given by[8]

$$\bar{E} = (E_1 \cos\alpha + E_4)/(1 + K\cos\alpha) , \quad (5)$$

where E_0 is the mean energy of the incident beam, E_1 is the mean energy of the front marker signal, $E_1 = K E_0$, E_4 is the mean energy of the rear marker signal, K is the elastic-scattering factor for the marker material ($K_{Pt} = 0.922$, $K_{Au} = 0.923$), and α is the scattering angle (less than 90°) measured with respect to the beam (= 12°) (see Fig. 1).

This average energy reduces to the arithmetic average of E_0 and E_4 if $\alpha = 0$ and $K = 1$ (corresponding to an infinitely heavy marker). When energy-straggling measurements are made by transmission, the average energy used is the arithmetic average of the mean incident-beam energy E_0 and the mean transmitted-beam energy (analogous to E_4 in a backscattering configuration). $\bar{E}$ is thus analogous to the average energy used in transmission experiments. The energy dependence of straggling is weak, however, and the definition of $\bar{E}$ has little influence on the results.

EXPERIMENTAL PROCEDURE

A. Sample preparation

Depositions were all made by electron-gun evaporation onto clean polished substrates in an oil-free vacuum system at pressures lower than 1×10^{-6} Torr. Dummy samples on vacuum-baked polished carbon substrates were prepared simultaneously with the targets. The dummies were used to check for light contaminants, such as oxygen, in the films. Film thicknesses were measured with a multiple-beam interferometer.

Ni samples were prepared by first depositing a Pt marker on a Si substrate and then annealing at 280 °C for about $\frac{1}{2}$ h in a dry N_2 atmosphere. The Pt reacts with the substrate and forms PtSi.[9] This prevents the Pt from mixing with Ni during the subsequent Ni evaporation. The Ni film and top marker were deposited sequentially without breaking vacuum.

Al samples were prepared by sequentially depositing onto Si or SiO_2 substrates a Au marker, an Al film, and a top Au marker without breaking vacuum. Precautions against mixing were not necessary, probably because small amounts of Al_2O_3 form in the initial stages of the Al evaporation, creating a diffusion barrier between Au and Al.

Au targets were prepared by evaporation of Au onto Si substrates.

The straggling measurements presented here were performed in a backscattering configuration with the 3.0 MeV Van de Graaf accelerator in the Kellogg Radiation Laboratory. The energy analysis of the backscattered particles was made using a Si surface barrier detector followed by a commercial preamplifier, linear amplifier, and multichannel analyzer.

B. Sample and apparatus evaluation

Since the quality of the samples is critical to straggling measurements, the samples were examined for defects which might lead to erroneous results. Among the properties investigated were contamination level, lateral uniformity, surface roughness, and temperature stability.

Contamination was checked by backscattering spectrometry on the dummy samples, and oxygen was found to be the chief contaminant. Other impurities were either lighter than C or present in concentrations too small to be detected (see Fig. 2). By far the highest oxygen contamination was found in the Al samples (typically 2 at.%). Contamination by oxygen at these concentrations, however, should not influence the straggling in any significant way.

To ascertain lateral uniformity, backscattering spectra taken from different parts of the sample were compared. The samples were found to be uniform within 2%.

The surface roughness was investigated with a scanning electron microscope. The surface of the sample appeared featureless. Any surface irregularities present were below the resoltuion of the microscope used (~400 Å). Surface roughness was not investigated further because previous investigations using a tally step (resolution ~ 100 Å) on Cr samples prepared similarly revealed that samples made on polished Si substrates were smooth to the order of the instrument resolution. Further indication that surface irregularities are small is given by the square root of thickness dependence of the straggling measurements, as it seems rather unlikely that surface roughness would significantly influence the measurements and leave the square root of thickness dependence unchanged.

The temperature stability of the films was investigated by annealing a completed target in a dry N_2 atmosphere for $\frac{1}{2}$ h at 200 °C. No change in the backscattering signal was noted.

Examination of the Al targets after irradiation

with an optical microscope revealed small blisters in the film. Their height was measured by Newton rings, and from estimates of their typical shape, size, and number it was determined that no significant errors were introduced in the straggling measurement by them. Al targets were also prepared on SiO_2 substrates and no blistering occurred on these samples. Data from both sets of samples are given in the results.

Experiments were made to investigate the possible influence on the measurements of carbon deposition on the target during irradiation, and of irradiation itself. To this end, spectra taken at various beam currents (5–50 nA) for various lengths of time (0.25–2 h) and with various beam sizes (1–10 mm^2) were compared with one another. No significant differences were observed in the straggling evaluated from these spectra.

The stability and linearity of the backscattering apparatus were checked by taking a backscattering spectrum of various elements ranging from C to Pt with the beam at a given energy E_0. The front-edge energy E_1 of each element can be expressed

$$E_1 = K_{\text{element}} E_0 \tag{6}$$

(see Fig. 1). If the beam energy is stable and the energy detection system is linear and stable, a plot of the calculated energy E_1 versus the channel number corresponding to the front-edge 50%-height point should yield a straight line. The apparatus was found to be sufficiently linear and stable (deviations $<0.5\%$ for irradiation times in excess of 18 h) to perform the straggling measurements. These last tests were performed *in situ* during straggling measurements for each set of samples.

THEORY

Several theories are available to describe energy straggling. The simplest is Bohr's theory,[10] according to which

$$\Omega_B^2 = (q^4/4\pi\epsilon_0^2) Z_1^2 N Z_2 \Delta R, \tag{7}$$

where q is the electronic charge, 1.60×10^{-19} C, $\epsilon_0 = 8.85\times10^{-12}$ F/m, Z_1 is the atomic number of the incident ion, Z_2 is the atomic number of the target material, ΔR is the ion path length, and N is the atom density of the target. Bohr's theory was derived assuming that (i) the target atoms are randomly distributed, (ii) the energy loss during a single interaction is very much less than the total energy loss over the entire path, and (iii) the projectile velocity is much greater than the orbital electron velocity of the target atoms. At low and medium energies this last assumption breaks down.

Lindhard and Scharff[11] have extended Bohr's theory by applying a correction factor for low- and medium-energy projectiles. Applying this correction, the energy straggling becomes

$$\begin{aligned} &\Omega_{LS}^2 = \Omega_B^2 \quad \text{for} \quad \omega = v^2/v_0^2 Z_2 > 3, \\ &\Omega_{LS}^2 = \Omega_B^2 (\tfrac{1}{2} L) \quad \text{for} \quad \omega \leq 3, \end{aligned} \tag{8}$$

where $v_0 = q^2/4\pi\epsilon_0 h$ is the electron velocity in the first Bohr orbital of a hydrogen atom, v is the velocity of the projectile, and L is the stopping number of the target material.

The value of L can be determined experimentally from the stopping cross section,

$$\epsilon_\alpha = (Z_1^2 q^4/4\pi\epsilon_0^2 m v^2) Z_2 L, \tag{9}$$

where ϵ_α is the stopping cross section of the target material α and m is the mass of the electron, 9.108×10^{-31} kg, or, based on the Thomas-Fermi model of the atom, L can be approximated by

$$L = 1.36\ \omega^{1/2} - 0.016\ \omega^{3/2}. \tag{10}$$

The last formula [Eq. (10)] was used in the calculation of Ω_{LS} (Fig. 6) so that the theory would be independent of ϵ_α. This is convenient since ϵ_α values quoted in the literature are uncertain; see, for instance, Ref. 15 with respect to Au.

A refinement of the Lindhard-Scharff calculation was made by Bonderup and Hvelplund.[12] This refinement assumes a spherically symmetric radial charge distribution, namely, the first-order Lenz-Jensen model.[13] Chu and Mayer[14] have made further refinements by introducing the Hartree-Fock-Slater model for the radial charge distribution into the formalism generated by Bonderup and Hvelplund. This calculation of Chu and Mayer shows the Z_2 oscillation characteristic of using the Hartree-Fock-Slater wave functions and has an energy dependence similar to that of the Lindhard-Scharff theory.

Applying Bohr's theory to the backscattering configuration yields [Eqs. (2) and (7)]

$$\Omega_{bB}^2 = K^2 \Omega_{B,\text{in}}^2 + \Omega_{B,\text{out}}^2 = \frac{q^4}{4\pi\epsilon_0^2} Z_1^2 N Z_2 \times \left(K^2 + \frac{1}{\cos\alpha}\right) \Delta R^*, \tag{11}$$

where ΔR^* is the thickness of the film.

In the remaining theories discussed, straggling is energy dependent. To calculate Ω_b with them, one can compute Ω_{in} and Ω_{out} independently at the average energy of each path and apply Eq. (2). Alternatively, one may calculate the straggling for the total path length, at the average energy $\bar{E}$ of Eq. (5). The result should be insensitive to the mode of calculation used because (i) the calculations are for thin targets, (ii) the calculations are for heavy targets or targets with heavy markers both

TABLE I. Measurements taken at a backscattering angle of 12° with a solid-state detector. Samples were made on Si substrates, with the exception of those marked +, which were made with SiO_2 substrates.

$\rho\Delta R^*$ (μg/cm^2)	E_0 (keV)	E_1 (keV)	E_4 (keV)	$\bar{E}$	ϵ_α	ΔE_1 (keV)	ΔE_4 (keV)	Ω (keV)
Al	$\rho = 2.7$ g/cm^3		$N = 6.0\times10^{22}$ atoms/cm^3				with Au markers	
32.96	2000	1846	1778	1883	47.93	18.84	22.77	5.44
59.08+	2000	1846	1726	1856	46.90	20.34	27.12	7.63
96.77	2000	1846	1649	1815	47.02	18.84	29.19	9.49
126.39+	2000	1846	1577	1778	48.89	19.44	33.22	11.46
32.96	1500	1385	1313	1411	50.67	18.48	23.35	6.04
59.08+	1500	1385	1253	1370	51.67	19.10	26.59	7.87
96.77	1500	1385	1165	1324	52.61	18.48	29.06	9.53
126.39+	1500	1385	1084	1282	55.16	19.90	33.29	11.36
32.96	1000	923	841	916	56.84	17.87	22.74	5.98
59.08+	1000	923	773	881	58.78	16.87	25.74	7.03
96.77	1000	923	677	830	66.95	18.44	28.60	9.30
Ni	$\rho = 8.9$ g/cm^3		$N = 9.13\times10^{22}$ atoms/cm^3				with Pt markers	
113.4	2000	1844	1688	1835	68.88	21.60	28.32	7.80
331.9	2000	1844	1381	1674	58.31	19.92	37.92	13.73
458.4	2000	1844	1213	1585	57.54	20.16	42.96	16.15
113.4	1500	1383	1220	1352	72.28	18.72	26.00	7.65
215.9	1500	1383	1062	1269	74.47	18.32	29.94	10.07
331.9	1500	1383	900	1184	72.90	18.12	32.51	11.48
458.4	1500	1383	743	1002	•••	18.52	38.81	14.50
215.9	1000	922	590	784	76.67	16.44	27.74	9.50
458.4	1000	922	443	707	71.90	16.87	31.17	11.15
Au	$\rho = 19.3$ g/cm^3		$N = 5.9\times10^{22}$ atoms/cm^3				no markers	
165.98	2000	1846	1737	1870	110.80	18.78	25.31	7.22
330.41	2000	1846	1621	1800	117.37	19.21	30.06	9.58
464.55	2000	1846	1526	1750	116.02	21.02	33.67	11.20
1180.00	2000	1846	923	1430	121.59	22.82	50.85	19.33
165.98	1500	1385	1266	1380	120.76	18.12	22.66	5.78
330.41	1500	1385	1143	1300	126.55	26.59	33.88	8.93
464.55	1500	1385	1037	1260	126.02	18.71	30.93	10.48
1180.00	1500	1385	506	978	125.28	22.51	49.77	18.89
165.98	1000	923	801	895	117.33	16.87	21.59	5.73
330.41	1000	923	676	830	128.81	16.87	26.03	8.42
464.55	1000	923	577	778	125.28	16.87	28.46	9.74

of which have incoming and outgoing paths in adjacent energy ranges, and (iii) the theoretical energy dependences are intrinsically weak. Nevertheless, both methods were used and the results were compared. The differences were found to be insignificant (< 0.05%), as expected.

RESULTS

Results of measurements are given in Table I and plotted in Figs. 3–5. Plotted along with the data are straggling values calculated using Bohr's theory. Figures 3–5 and Table I are presented using areal density $\rho\Delta R^*$ where ρ is the bulk density, rather than the thickness ΔR^*. This was done to conform with presentations used in the bulk of the literature.

Energy straggling in all three elements is roughly proportional to square root of thickness, as predicted by Bohr. Measurements in Ni roughly agree with the Bohr theory, while in Al they are about 30% above and in Au about 40% below this theory.

The Au measurements are similar to previous measurements made in Pt.[6] This was expected since Pt and Au are neighboring elements in the periodic table. The straggling results in Al are similar to the results of Demichelis[4] and Sykes,[5] whose values are also higher than Bohr's theory. However, their data apply to much thicker films (~ mg/cm^2) and higher energies (~5 MeV), so that direct comparison is somewhat difficult. The situation is similar for Ni in that previous measurements[3] have been made at much higher energies and with thicker films.

In order to display the energy dependence of straggling it is convenient to plot $\Omega(NZ_2\Delta R^*)^{1/2}$, since this reduces Bohr's theory to a universal curve. Figure 6 displays $\Omega(NZ_2\Delta R^*)^{1/2}$ vs $\bar{E}$ for all three elements and the theories of Bohr,[10]

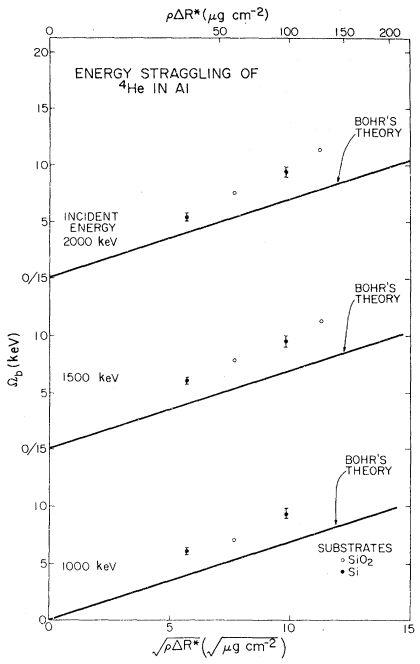

FIG. 3. Energy straggling of ^{4}He in Al films at incident energy of 1000, 1500, and 2000 keV as a function of the square root of areal density $\rho\Delta R^*$, where ΔR^* is the film thickness and ρ is the density. Solid line shows predictions of Bohr's theory.

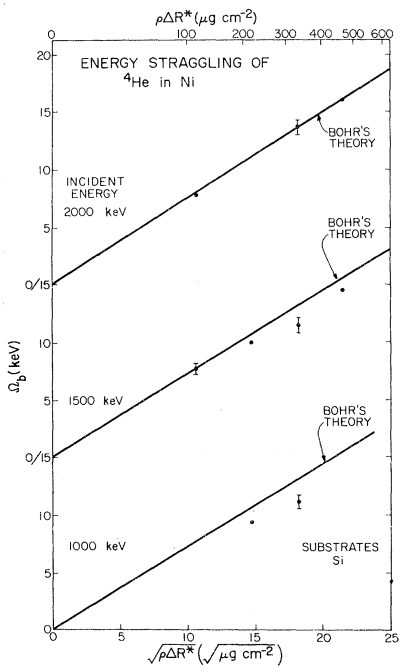

FIG. 4. Energy straggling of ^{4}He in Ni films at incident energy of 1000, 1500, and 2000 keV as a function of the square root of areal density $\rho\Delta R^*$, where ΔR^* is the film thickness and ρ is the density. Solid lines show predictions of Bohr's theory.

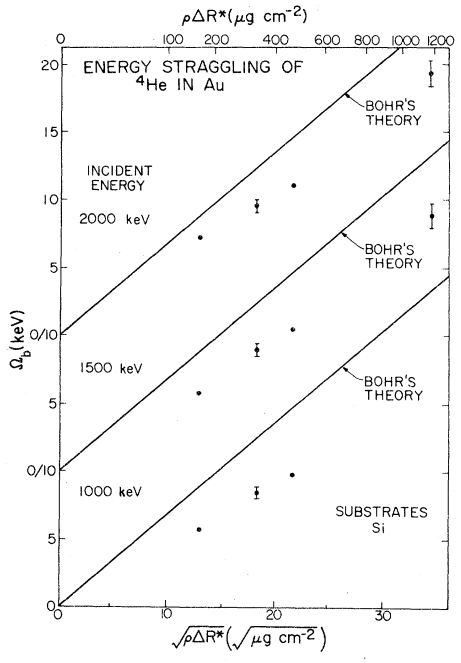

FIG. 5. Energy straggling of ^{4}He in Au films at incident energy of 1000, 1500, and 2000 keV as a function of the square root of areal density $\rho\Delta R^*$, where ΔR^* is the film thickness and ρ is the density. The solid line shows predictions of Bohr's theory.

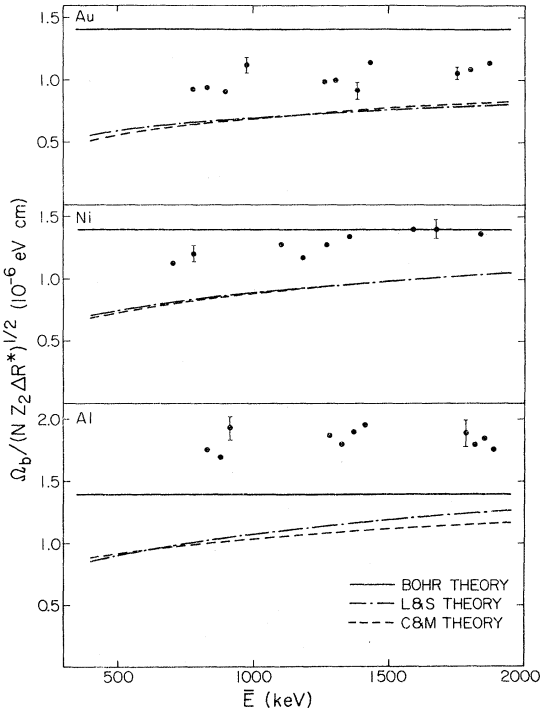

FIG. 6. Normalized straggling of ^{4}He in Al, Ni, and Au vs average energy, including the theories of Bohr (Ref. 10), Lindhard and Scharff (Ref. 11), and Chu and Mayer (Ref. 14).

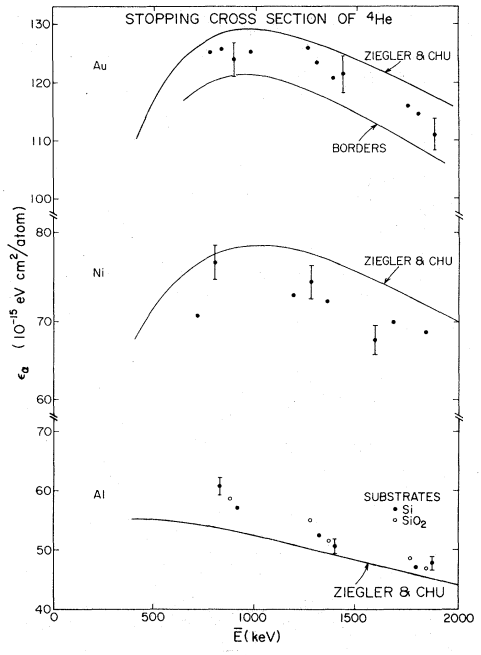

FIG. 7. Stopping cross section as a function of average energy for Al, Ni, and Au. Solid lines are values taken from Ziegler and Chu (Ref. 15) and Borders (Ref. 15).

Lindhard and Scharff,[11] and Chu and Mayer.[14] These last two theories qualitatively describe the observed energy dependence of straggling. However, the predictions of both theories are below the measurements for all three elements. Based on the data presented, it is not clear which theory gives the most accurate description of energy straggling.

The main statistical error in these measurements originates from the energy differences ΔE_1 and ΔE_4, which cannot be determined to better than ± 2.0 keV. This error, when added in quadrature with smaller statistical errors and propagated, yields an estimated uncertainty of about 10% in Ω. Representative error bars are given for Ω in Figs. 3–5. Error bars for the thickness are omitted in these figures since the resulting uncertainty in the abscissa (~2.5%) is typically the size of the symbol used.

To check for systematic errors in the measurements, ϵ_α was calculated from the backscattering spectra[8] and compared with current values in the literature.[15] Both the literature values and those from the backscattering spectra are shown in Fig. 7. The error bars given here arise from uncertainties in E_1, E_4, and the thickness of the films (~6% total). This check revealed no significant systematic errors since ϵ_α agrees with literature values within about 8% on the average.

CONCLUSION

Energy straggling of ^{4}He ions in Al, Ni, and Au, for the energy range of this experiment is roughly proportional to square root of thickness, as predicted by Bohr's theory. While Ni measurements are in fair agreement with this theory, Al measurements are about 30% above and Au measurements about 40% below predicted values. A weak dependence in straggling for these elements is qualitatively described by the theories of Lindhard and Scharff, and Chu and Mayer. These latter two theories underestimate the straggling in all three elements.

ACKNOWLEDGMENTS

We are grateful to J. S. Feng for supplying some samples and suggesting the use of markers and would like to thank W. K. Chu for providing his theoretical calculations. We also appreciate the assistance of D. S. Harris, M. E. Rienstra, and L. G. Scroggs in the preparation of the manuscript.

†Work supported by the Office of Naval Research (L. Cooper).

[1]W. K. Chu, J. W. Mayer, M-A. Nicolet, T. M. Buck, G. Amsel, and F. Eisen, Thin Solid Films 17, 1 (1973).
[2]C. B. Madsen and P. Venkatesworlu, Phys. Rev. 74, 1782 (1948); C. B. Madsen, K. Dan. Vidensk. Selsk. Mat.-Fys. Medd. 27, 13 (1953); L. P. Nielsen, *ibid.* 33, 6 (1961).
[3]J. R. Comfort, J. E. Decker, E. T. Lynk, M. O. Scully, and A. R. Quinton, Phys. Rev. 150, 249 (1966).
[4]F. Demichelis, Nuovo Cimento 13, 2134 (1959).
[5]D. A. Sykes and S. J. Harris, Nucl. Instrum. Methods 94, 39 (1971).
[6]J. M. Harris, W. K. Chu, and M-A. Nicolet, Thin Solid Films 19, 259 (1973).
[7]L. Landau, J. Phys. 8, 201 (1944); C. Tschalär, Nucl. Instrum. Methods 61, 141 (1968); J. J. Kolata, Phys. Rev. 176, 484 (1968).
[8]R. D. Moorhead, J. Appl. Phys. 36, 391 (1965); W. D. Warters, Ph. D. dissertation (Caltech, 1953) (unpublished).
[9]A. Hiraki, M-A. Nicolet, and J. W. Mayer, Appl. Phys. Lett. 18, 178 (1971).
[10]N. Bohr, K. Dan. Vidensk. Selsk. Mat.-Fys. Medd. 18, 8 (1948).
[11]J. Lindhard and M. Scharff, K. Dan. Vidensk. Selsk. Mat. Fys. Medd. 27, 15 (1953).
[12]E. Bonderup and P. Hvelplund, Phys. Rev. A 4, 562 (1971).
[13]H. Jensen, Z. Phys. 77, 702 (1932).
[14]W. K. Chu and J. W. Mayer (unpublished).
[15]J. F. Ziegler and W. K. Chu (unpublished); Thin Solid Films 19, 281 (1973); J. A. Borders, Radiat. Eff. 16, 253 (1972).